Ligand-Enabled Oxidative Fluorination of Gold(I) and Light-Induced Aryl–F Coupling at Gold(III)

David Vesseur, Shuo Li, Sonia Mallet-Ladeira, Karinne Miqueu, Didier Bourissou

Ligand-Enabled Oxidative Fluorination of Gold(I) and Light-Induced Aryl–F Coupling at Gold(III)

David Vesseur,[1] Shuo Li,[1] Sonia Mallet-Ladeira,[2] Karinne Miqueu,[3] Didier Bourissou[1]*

[1] CNRS/Université Paul Sabatier
Laboratoire Hétérochimie Fondamentale et Appliquée (LHFA, UMR 5069)
118 Route de Narbonne, 31062 Toulouse Cedex 09 (France)
E-mail: didier.bourissou@univ-tlse3.fr

[2] Institut de Chimie de Toulouse (UAR 2599)
118 Route de Narbonne, 31062 Toulouse Cedex 09 (France)

[3] CNRS/Université de Pau et des Pays de l'Adour
E2S-UPPA, Institut des Sciences Analytiques et de Physico-Chimie pour l'Environnement et les Matériaux (IPREM, UMR 5254)
Hélioparc, 2 Avenue du Président Angot, 64053 Pau Cedex 09 (France).

ABSTRACT: MeDalphos Au(I) complexes featuring aryl, alkynyl and alkyl groups readily react with electrophilic fluorinating reagents such as *N*-fluorobenzenesulfonimide and Selectfluor. The ensuing [(MeDalphos)Au(R)F]$^+$ complexes have been isolated and characterized by multi-nuclear NMR spectroscopy as well as X-ray diffraction. They adopt a square-planar contra-thermodynamic structure, with F *trans* to N. DFT/IBO calculations show that the N lone pair of MeDalphos assists and directs the F^+ transfer to gold. The [(MeDalphos)Au(Ar)F]$^+$ (Ar = Mes, 2,6-F_2Ph) complexes smoothly engage in C–C cross-coupling with PhCCSiMe_3 and Me_3SiCN, providing direct evidence for the oxidative fluorination/transmetalation/reductive elimination sequence proposed for F^+-promoted gold-catalyzed transformations. Moreover, direct reductive elimination to forge C–F bond at Au(III) was explored and substantiated. Thermal means proved unsuccessful, leading mostly to decomposition, but irradiation with UV-visible light enabled to efficiently promote aryl–F coupling (up to 90% yield). The light-induced reductive elimination proceeds under mild conditions, it works even with the electron-deprived 2,6-difluorophenyl group and it is not limited to the contra-thermodynamic form of the aryl Au(III) fluoride complexes.

Introduction

While Au(I)/Au(III) redox catalysis was long considered as an overwhelming challenge due to the reluctance of Au(I) to undergo oxidation to Au(III),[1] many catalytic cycles involving this elementary step have been reported over the past fifteen years. These transformations have become possible thanks to three distinct methodologies developed to promote Au(I) to Au(III) oxidation. The first catalytic Au(I)/Au(III) cycles made use of stoichiometric amounts of external oxidants such as "F^+" surrogates or hypervalent I(III) derivatives.[2,3] Then, the use of photo redox conditions with or even without external

photocatalyst also proved to be efficient and very powerful.[4] Lastly, our group introduced a complementary ligand-based approach where chelating/hemilabile ligands trigger oxidative addition to gold.[5,6] While the mechanisms and key factors at play for I(III), photoredox and ligand-enabled transformations have been studied quite extensively and are now relatively well understood, this is not the case for the "F^+" route involving reagents such as Selectfluor or *N*-fluorobenzenesulfonimide (NFSI). Given the lack of direct experimental evidence, the mechanisms proposed for these catalytic transformations are only based on indirect observations. Accordingly, it is commonly suggested that the fluorinating reagents first oxidize linear gold(I) precursors by formal transfer of F^+ and a weakly coordinating anion. The ensuing Au(III) fluoride complexes[3a,7] are coordinatively unsaturated and thus highly reactive (Figure 1a). This high reactivity on one hand allows for facile fluorine-assisted transmetalation followed by reductive elimination to give C–C coupling products, but on the other hand, it has prevented isolation or even spectroscopic characterization of the Au(III) fluoride intermediates.

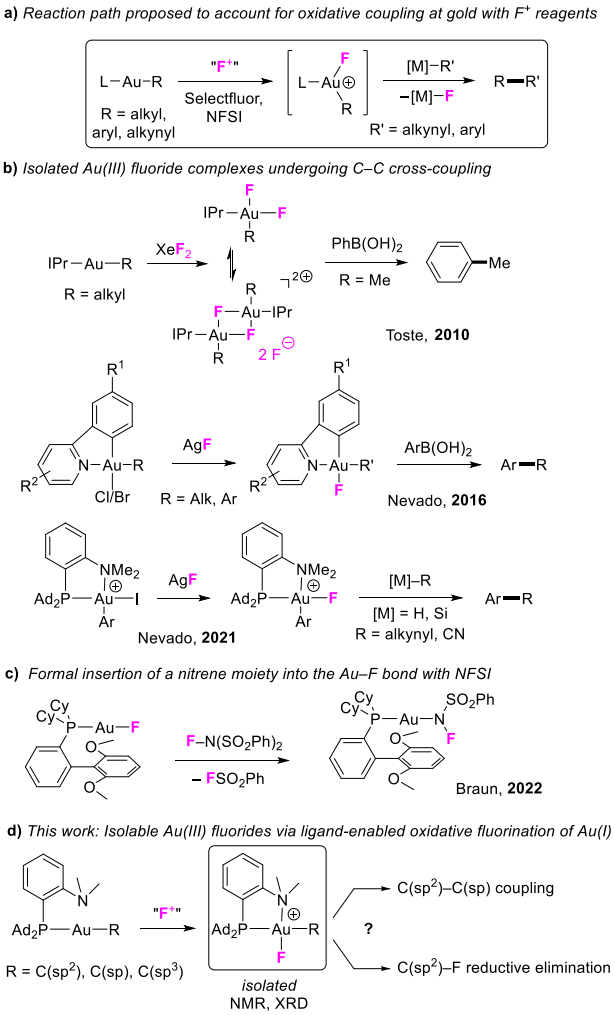

Figure 1. a) Reaction path commonly proposed to account for gold-catalytic cross-coupling reactions in the presence of electrophilic fluorinating reagents. b) Isolated Au(III) fluoride complexes shown to engage in fluorine-

assisted transmetalation followed by reductive elimination. c) Reaction of a Au(I) fluoride with NFSI. d) Ligand-enabled oxidative fluorination of Au(I) complexes resulting in isolable Au(III) fluorides that undergo fluorine-assisted transmetalation and $C(sp^2)$–F reductive elimination.

Different strategies have been developed to circumvent the challenges associated with the highly reactive three-coordinate Au(III) fluoride intermediates. First, Toste and co-workers reported in 2010 the oxidation of NHC Au(I) alkyl complexes with the extremely strong oxidant XeF_2 (Figure 1b).[8-10] The formed alkyl Au(III) difluoride complexes were found to be in equilibrium between monomeric and dimeric forms (*via* dissociation of one fluoride and μ_2-bridging of the remaining fluoride). The methyl Au(III) complex proved active in fluorine-assisted transmetalation with aryl boronic acids followed by reductive elimination resulting in $C(sp^2)$–$C(sp^3)$ coupling.[8] Fluorine-assisted transmetalation and $C(sp^2)$–$C(sp^2)$/C(sp) coupling from Au(III) fluorides have been further investigated by Nevado and co-workers with (C,N)-cyclometalated and (P,N)-chelated complexes.[11-13] These Au(III) fluoride precursors were synthetized using an alternative approach, *i.e.* halide exchange at Au(III) using AgF.[11-14]

It is striking to note that the reactivity of Au(III) fluoride complexes towards transmetalation/reductive elimination has been thoroughly studied, whereas the electrophilic oxidation of Au(I) with mild oxidative fluorinating reagents, as proposed in catalytic cycles, remains elusive. We are aware of a single example involving a peculiar T-shaped Au(I) complex featuring a CNC pincer ligand.[15] As mentioned above, it is most likely the coordinatively unsaturated nature of the $[LAu(R)F]^+$ complexes which makes them so reactive and thus difficult to be directly characterized and studied. A recent study by Braun and co-workers is very representative of this situation. Indeed, upon reaction with NFSI, the (SPhos)AuF complex underwent a formal nitrene insertion in the Au–F bond, resulting in a Au(I) fluoroamino complex (Figure 1c).[16] This reaction proceeded at temperature as low as –60 ºC and no intermediate could be detected.

Given the exceptional proficiency hemilabile ligands, in particular MeDalphos, have demonstrated in oxidative addition to Au(I),[6] and Au(I) to Au(III) oxidation,[17] we imagined they may also be fruitful to access, stabilize and study Au(III) fluoride complexes (Figure 1d). Here we report that the hemilabile MeDalphos ligand indeed enables the oxidative fluorination of Au(I) complexes. The ensuing Au(III) fluorides are stabilized by coordination of the pendant nitrogen centre which allows for their isolation and full characterization including by X-ray diffraction analysis. The organic group at gold and the fluorinating reagent have been varied to assess the scope of the reaction. The oxidative fluorination process has also been investigated in-depth by DFT/IBO calculations, providing insight into the F^+ transfer to gold. The thereby obtained Au(III) fluorides were found to readily undergo fluorine-assisted transmetalation

followed by reductive elimination, demonstrating their value as model substrates for oxidative Au(I)/Au(III) catalytic C–C cross-couplings. Additionally, we discovered that highly challenging C(sp^2)–F reductive eliminations can be efficiently triggered by irradiation with UV-visible light.

Results and discussion

Oxidative fluorination of Au(I). The experimental studies were started with *N*-fluorobenzenesulfonimide (NFSI) as well-soluble mild oxidative fluorinating reagent and the phenyl-substituted (MeDalphos)AuPh complex as the Au(I) precursor, which could be readily prepared from (MeDalphos)AuCl and $PhB(OH)_2$ or PhLi (Scheme 1).[18] Right after mixing the two at room temperature in DCM, ^{31}P NMR spectroscopy showed a noticeable change, from a singlet at δ 60.8 ppm to a doublet at δ 64.2 ppm with coupling to fluorine (J_{FP} = 7.3 Hz). Oxidation to Au(III) and coordination of the nitrogen atom of the (MeDalphos) ligand are apparent from the ^1H NMR spectrum where the $N(CH_3)_2$ resonance has shifted from δ 2.66 ppm to 3.56 ppm.[5c,e,g] In addition, ^{19}F NMR spectroscopy shows a doublet at δ –299.6 ppm with coupling to phosphorus (J_{FP} = 7.3 Hz). The ^{19}F NMR chemical shift of **1a** falls in the lower range of those found previously for Au(III) fluoride complexes (δ from –150 to –320 ppm typically).[8-15] The small value found for J_{FP} contrasts with the large coupling constants observed for the analogous [(MeDalphos)Au(Ar)F]$^+$ complexes with fluorine *trans* to phosphorus (J_{PF} ~ 100 Hz).[12] This suggests that the oxidative fluorination occurs *trans* to nitrogen which can assist in the oxidation of the gold centre (this assertion is supported by DFT calculations, *vide infra*), and thus the aryl remains *trans* to phosphorus. Such ligand-assisted oxidative fluorination of Au(I) is reminiscent of the *o*-phenanthroline-assisted oxidation of Pd(II) complexes into Pd(IV) fluorides reported recently by Ritter and coworkers.[19] It is noteworthy that the fluorine sits *trans* to nitrogen in **1a** despite nitrogen providing a lower thermodynamic *trans* influence compared to phosphorus.[20] Thus, complex **1a** adopts a "contra-thermodynamic" structure. The relative stability of the two isomers has been ascertained computationally, *vide infra*.

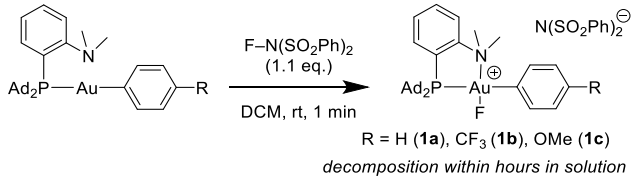

Scheme 1. Oxidative fluorination of (MeDalphos)AuAr complexes with NFSI in DCM.

Upon NMR monitoring, the signals of **1a** were found to disappear within an hour at room temperature, indicating decomposition and preventing isolation as well as full characterization. In an attempt to stabilize the proposed Au(III) fluoride complex, the electronic nature of the aryl substituent at gold was modified. Electron-withdrawing (CF_3, **1b**) and electron-donating (OMe, **1c**) groups were tried. In both cases, a doublet around δ –300 ppm with small coupling constant (J_{FP} < 10 Hz) was observed by ^{19}F NMR spectroscopy, but it again vanished within an hour at room temperature, as for the parent phenyl complex **1a**, suggesting that the electronic nature of the aryl ring does not significantly affect the stability of the Au(III) fluoride complex. To probe the stability of the Au(III)–F complexes in different solvents, the reaction of (MeDalphos)AuPh with NFSI was repeated in more coordinating solvents (MeCN and THF). This did not result in a significant change in the lifetime of complex **1a**. Finally, the reaction was performed in toluene and Et_2O. Here, the cationic complex rapidly precipitated after addition of NFSI. When the reaction was performed in toluene at 5 °C, the Au(III)–F complexes **1a-d** could be isolated in 85-99% purity (according to ^{19}F, ^{31}P and ^{1}H NMR spectroscopy) after removal of the solvent (Scheme 2). Subsequent dissolution of the isolated Au(III) fluorides at low temperature (–60 °C) allowed for complete characterization by multi-nuclear NMR.[18] The isolated complexes **1a-d** can be stored in a glovebox for several weeks at room temperature without any significant change in purity being detected.

The scope of the reaction was then extended to *ortho*-substituted aryl groups. The mesityl substituted complex **1e** was obtained in excellent yield (95%). In contrast to non-*ortho*-substituted derivatives **1a**-**1d**, complex **1e** proved to be stable in solution at room temperature, without any observable decomposition occurring after 24 hours in MeCN. Similar increase in stability was observed for the other *ortho*-substituted compounds **1f** and **1g**, with only minor decomposition at room temperature detected after 24 hours in MeCN. These observations confirm that the electronic nature of the aryl ring at gold does not play a major role in stabilizing the Au(III) fluoride. The key seems to be steric protection around the Au–F bond. When increasing the sterics around the Au centre even further with *ortho* isopropyl groups, a higher reaction temperature was required (25 instead of 5 °C), after which **1h** was isolated with a lowered yield of 45%. Mono *ortho*-substituted **1i** and **1j** also displayed good stability with only minor decomposition after 24 hours at room temperature in MeCN, showing that even a single *ortho* substitution increases significantly the stability of the Au(III) fluoride complex.

Finally, the scope of the reaction was expanded to alkyl and alkynyl substituents. Both **1k** and **1l** featuring alkyl substituents display great stability despite the lack of steric protection around gold and fluorine. The alkynyl-substituted complex **1m** could also be prepared in good yield, with complete selectivity for the fluorination of gold over the C≡C triple bond. It is worth noting that Au(III)–F alkynyl complexes have been proposed as intermediates in catalytic reactions involving oxidative fluorination,

but have never been observed experimentally before **1m**.[21] The hemilabile MeDalphos ligand thus enables oxidative fluorination of a variety of Au(I) precursors bearing sp, sp^2 and sp^3-hybridized organic groups, and it stabilizes the ensuing Au(III) fluoride complexes by chelation.

The oxidative fluorination of the (MeDalphos)AuR complexes proceeds efficiently with NFSI. This raises the question about other common oxidative fluorinating reagents. The generality of the transformation was assessed on the thermally stable mesityl complex **1e** (Scheme 3). The reaction of (MeDalphos)AuMes with *N*-fluoro pyridinium resulted in the Au(III) fluoride complex **1e-BF$_4$** in excellent yield based on ^{19}F NMR spectroscopy (over 95%). The complex could be isolated as a pure solid in 75% yield. The 2,6-chlorinated *N*-fluoro pyridinium also afforded the Au(III) fluoride **1e-BF$_4$** albeit in significantly lower yield (43%). Selectfluor worked particularly well resulting in **1e-BF$_4$** in quantitative yield, similar to NFSI. While the Au centre undergoes oxidation devoid of any discernible side product formation, as indicated by ^{19}F NMR spectroscopy, the Au(III) fluoride complex was not isolated as it proved difficult to separate from the triethylenediamine by-product. Finally, the extremely strong oxidizing agent XeF_2 used previously by Toste[8,9] and Menjon[9] was tested. Here also, the oxidation proceeded selectively resulting in the Au(III) fluoride **1e-Cl** in good isolated yield (77%). Apart from the signals associated with the counteranions, the spectroscopic data of complexes **1e**, **1e-BF$_4$** and **1e-Cl**[14d] were found to be essentially identical. It is thus likely that the counteranion remains spectator and does not coordinate to the Au(III) centre, independently of whether the anion is coordinating (Cl^-), weakly coordinating ($N(SO_2Ph)_2^-$) or non-coordinating (BF_4^-).

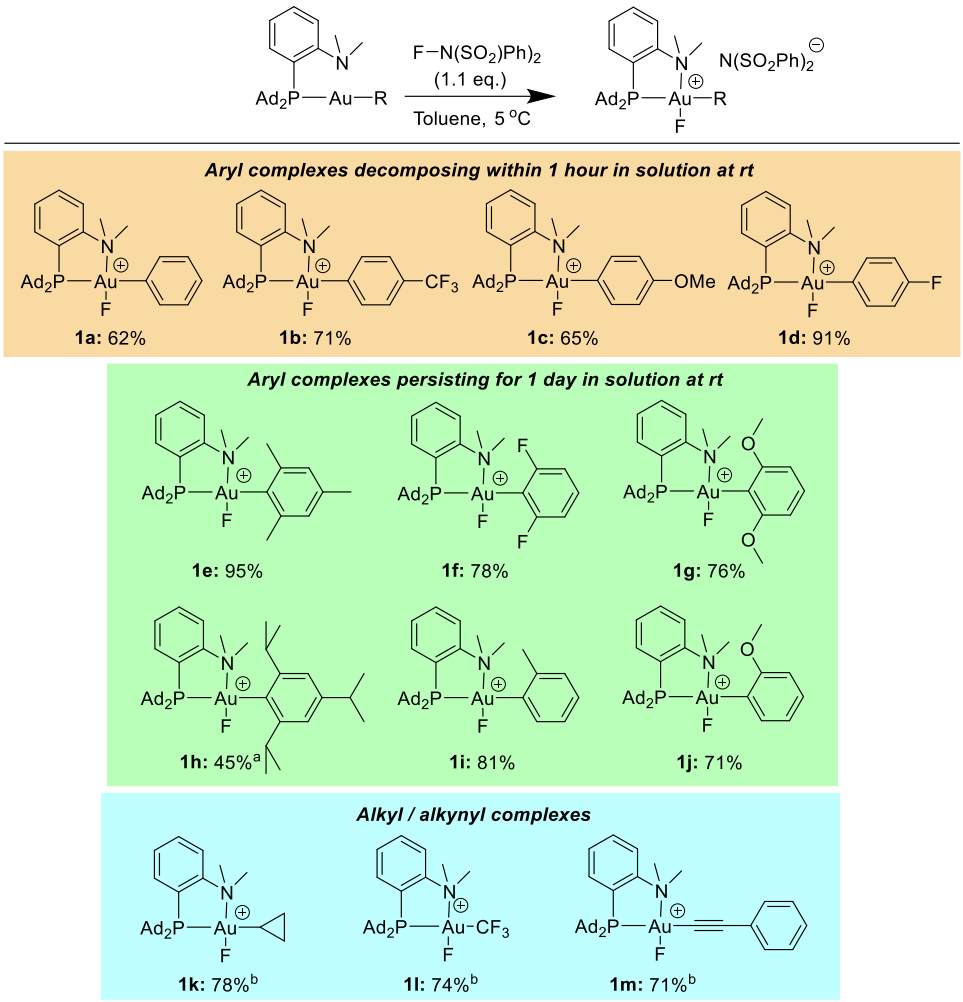

Scheme 2. Synthesis of Au(III) fluoride complexes, with isolated yields. [a]Reaction carried out at room temperature. [b]Reaction carried out in Et_2O for 1 hour at room temperature.

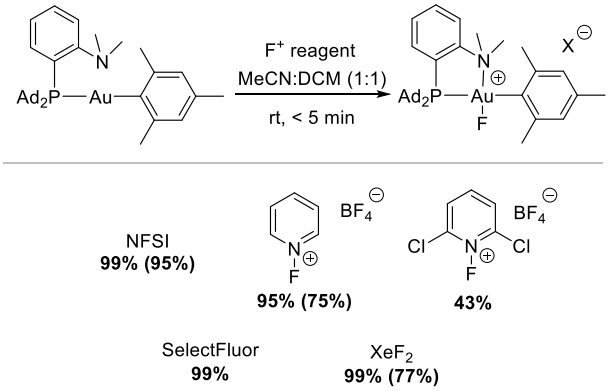

Scheme 3. Oxidative fluorination of (MeDalphos)AuMes with different oxidative fluorination reagents. Yields based on ^{19}F NMR spectroscopy with $PhCF_3$ as internal standard. Isolated yields in brackets.

As previously discussed, the spectroscopic data provided very strong support for the formation of Au(III) fluorides with the fluor *cis* to phosphorus. Complementary and definite proof for the formation of these "contra-thermodynamic" complexes was readily obtained with **1f** and **1i** for which crystals suitable for X-ray diffraction analysis directly crashed down from the reaction mixture. Additionally, crystals could be grown by vapor diffusion of pentane into a concentrated *ortho*-dichlorobenzene solution of **1e**. The thereby determined solid-state structures unambiguously confirm the formation of the "contra-thermodynamic" Au(III) fluoride complexes (Figure 2).[18] The three compounds adopt square-planar geometry with coordination of the nitrogen to the Au(III) centre (Au–N = 2.057 to 2.119 Å) and the fluorine sitting *trans* to nitrogen. The Au–F bond distance (1.903 to 1.941 Å) is shorter by 0.1 to 0.2 Å compared to the previously reported F *trans* to P [(MeDalphos)Au(Ar)F]$^+$ isomers (2.006 to 2.133 Å), in line with the lower *trans* influence of N compared to P.[20] The Au–F bond length decreases when going from the electron-deprived species **1f** (Au–F = 1.941 Å) to the electron-enriched ones **1e** (Au–F = 1.916 Å) and **1h** (Au–F = 1.903 Å), a trend also observed with the F *trans* to P isomers.[12]

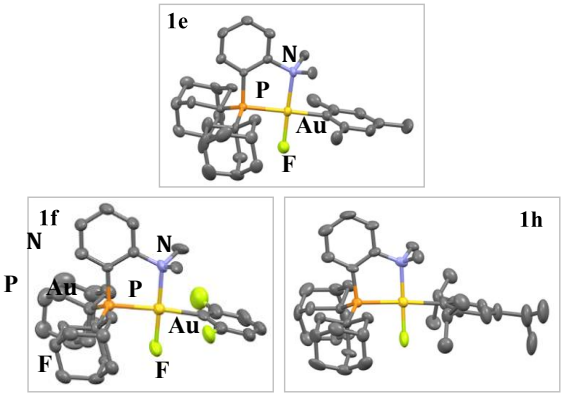

Figure 2. Molecular structures of the (P,N)-ligated Au(III) fluoride complexes 1e, 1f and 1h. For sake of clarity, the anions and hydrogen atoms are omitted. Ellipsoids are shown at 50% probability. Selected bond distances (in Å) and angles (in °): for 1e, P–Au 2.357(2), N–Au 2.119(6), Au–C 2.086(7), Au–F 1.916(4), P–Au–F 94.4(1), P–Au–N 86.8(1), C–Au–N 94.4(2), C–Au–F 84.4(2); for 1f: P–Au 2.335(2), N–Au 2.100(8), Au–C 2.11(5), Au–F 1.941(6), P–Au–F 91.7(2), P–Au–N 87.9(2), C–Au–N 97(1), C–Au–F 84(1); for 1h: P–Au 2.353(3), N–Au 2.076(7), Au–C 2.094(9), Au–F 1.903(5), P–Au–F 92.39(17), P–Au–N 87.1(2), C–Au–N 95.7(3), C–Au–F 84.8(3).

Computational investigations. DFT calculations have been carried out at the SMD(MeCN)-B3PW91-D3(BJ)/SDD+f(Au),6-31G**(other atoms)//B3PW91-D3(BJ)/SDD+f(Au),6-31G**(other

atoms) level of theory in order to assess the relative stability of the *cis*/*trans* forms of the [(MeDalphos)Au(Ar)F]$^+$ complexes, and to shed light into the way the F^+ transfer from the electrophilic fluorinating reagents to Au proceeds and how the MeDalphos ligand directs it. Relative stability of the cis/trans forms. First, computations were performed on complexes **1e**, **1f** and **1h** in their "contra-thermodynamic" form to compare with the X-ray data. The optimized geometries match well with those determined crystallographically (Figure S3),[18] with only small differences in the key structural parameters (maximum deviation in the Au–P, Au–N, Au–F and Au–C bond lengths < 0.04 Å). The theoretical study was then extended to complexes **1a-d** and **1i**. The comparison of the optimized geometries of the two isomeric structures, with F trans to N or trans to P, shows similar trends as for the XRD data. The Au–F bond is slightly shorter when exposed to the weaker trans influence of N compared to P (~ 1.94–1.95 Å in the "contra-thermodynamic" form with F trans to N vs 1.98–1.99 Å in the thermodynamic form with F trans to P).[18,20] In all cases, the F trans to N isomer is found higher in energy than the F trans to P isomer (Figures 3, S3 and S4),[18] confirming that oxidative fluorination affords the Au(III) fluoride complex in "contra-thermodynamic" form. The difference in energy between the two isomers is sizeable and does not vary very much (at least 12.2 kcal/mol and 16.9 kcal/mol maximum in the gas phase). For the non-substituted complex **1a**, the energy difference is 15.3 kcal/mol. In the para-X substituted series **1b-d** (X = F, OMe, CF_3), the energy gap remains about constant (from 15.3 to 16.8 kcal/mol), indicating that electronic effects have only marginal impact. For the mesityl and 2,6-difluorophenyl complexes **1e** and **1f**, the difference in energy decreases slightly (to 12.2 and 14.0 kcal/mol, respectively). Here, the steric repulsion between the aryl group at Au and the Ad groups at P may come into play to destabilize the F trans to P isomer. The NMe_2 group is much less sterically demanding than the PAd_2 moiety and better accommodates sterically demanding aryl groups in cis position. It is however difficult to discern a general trend as larger energy gaps were found for complexes **1h** and **1i** bearing 2,4,6-trisisopropylphenyl and ortho-tolyl groups (16.7 and 16.9 kcal/mol, respectively).

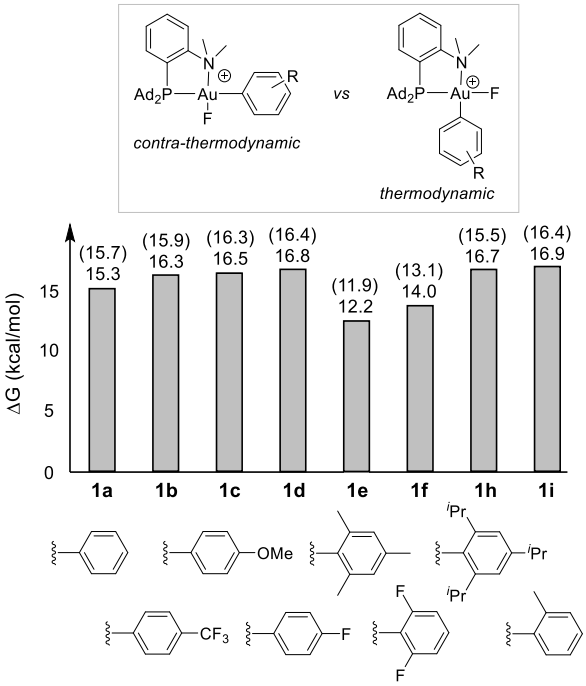

Figure 3. Relative energy (ΔG in kcal/mol) of the thermodynamic and contra-thermodynamic forms of the $[(MeDalphos)Au(Ar)F]^+$ complexes (F *trans* to P and N, respectively) computed at the B3PW91-D3(BJ)/SDD+f(Au), 6-31G** (other atoms) level of theory. Values at SMD(DCM)-B3PW91-D3(BJ)/SDD+f(Au), 6-31G** (other atoms)//B3PW91-D3(BJ)/ SDD+f(Au), 6-31G** (other atoms) are given in brackets.

Ligand-enabled oxidative fluorination of gold. The F^+ transfer to the Au(I) complex (MeDalphos)AuMes was then investigated. The energy profile computed with NFSI as fluorinating reagent at the SMD(DCM)-B3PW91-D3(BJ)/SDD+f(Au),6-31G** (other atoms) // B3PW91-D3(BJ)/SDD+f(Au),6-31G** (other atoms level of theory is displayed in Figure 4. The transformation is highly exergonic (ΔG –32.8 kcal/mol). It proceeds in a single step with a small activation barrier ($\Delta G^{\neq}$ 6.5 kcal/mol). Its transition state shows quasi linear Au–F–$N(SO_2Ph)_2$ arrangement (165.5°) with fluorine approaching gold (Au•••F 2.364 Å) in *trans* position to the N atom of the MeDalphos ligand. Selectfluor was also considered as fluorinating reagent. The corresponding energy profile is given in Figure S5.[18] The activation barrier is slightly lower than for NFSI ($\Delta G^{\neq}$ 4.8 kcal/mol), in agreement with Selectfluor being a stronger oxidant and reacting faster with **1e** than NFSI. In this case, the transition state is very early. The Au•••F distance is long (3.076 Å) and the Au–F–N skeleton is strongly bent (119.1°).

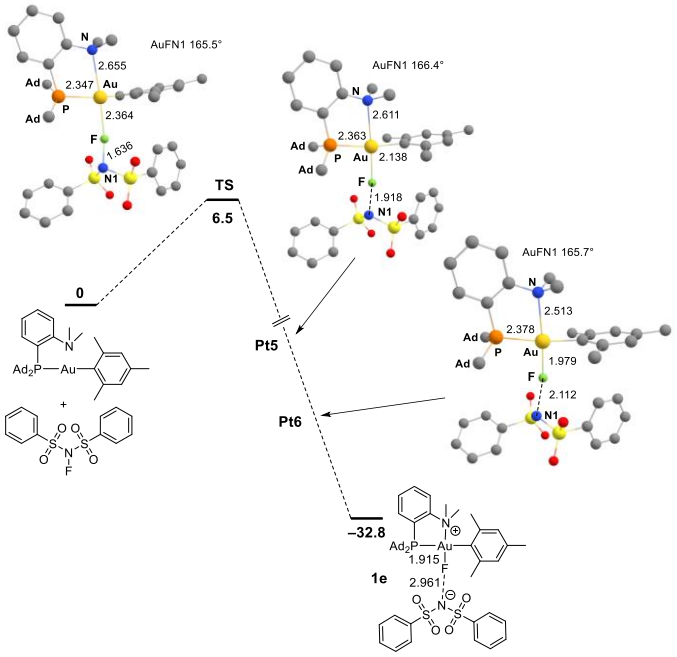

Reactants	TS	Pt5	Pt6	Product
AuF 2.849	**AuF** 2.364	**AuF** 2.138	**AuN** 1.979	**AuF** 1.915
AuN 2.802	**AuN** 2.655	**AuF** 2.611	**AuN** 2.513	**AuN** 2.177
d_{Au} Au 1.957	$d_{Au} \rightarrow \sigma^*_{N1F}$ Au 1.725 F 0.07 N1 0.154	$d_{Au} \rightarrow \sigma^*_{N1F}$ Au 1.485 F 0.06 N1 0.301	$d_{Au} \rightarrow \sigma^*_{N1F}$ Au 0.410 F 1.417 N1 0.03	σ_{AuF} Au 0.390 F 1.491
n_N N 1.832	n_N N 1.769	$n_N \rightarrow Au$ N 1.705 Au 0.05	$n_N \rightarrow Au$ N 1.668 Au 0.162	σ_{AuN} N 1.582 Au 0.282
σ_{N1F} F 1.226 N1 0.752	σ_{N1F} F 1.231 N1 0.706	σ_{N1F} Au 0.095 F 1.342 N1 0.471	σ_{N1F} Au 0.159 F 0.03 N1 1.511	n_{N1} N1 1.663

Figure 4. Energy profile (ΔG in kcal/mol) for the F^+ transfer from NFSI to the (MeDalphos)AuMes complex computed at the SMD(DCM)-B3PW91-D3(BJ)/SDD+f(Au), 6-31G** (other atoms)//B3PW91-D3(BJ)/SDD+f(Au),6-31G** (other atoms) level of theory. Intrinsic Bond Orbital (IBO) analysis along the reaction profile. Main distances in Å and bond angles in °. For the IBOs, the fractions of electrons of the doubly occupied orbitals assigned to each

atom are given. Pt5 and Pt6 refer to structures on the Intrinsic Reaction Coordinate between which the electronic redistribution occurs and F^+ is formally transferred from N to Au. For clarity, the hydrogen atoms and adamantyl (Ad) groups are omitted in the energy profile, only the H atoms are omitted in the IBO plots.

To gain more insight into the F^+ transfer to Au, Intrinsic Bond Orbital (IBO) analyses[22] were carried out along the intrinsic reaction coordinate (IRC). With both fluorinating reagents, the electronic redistribution and oxidative fluorination of gold were found to occur after the transition state. For NFSI (Figure 4), it happens when the Au–F distance reaches ~ 2.0 Å (between **Pt5** and **Pt6** on the IRC, Figure S6).[18] The $d_{x^2-y^2}$(Au) orbital of the (MeDalphos)AuMes complex progressively transforms into a σ_{AuF} orbital while the N1–F σ-bond of NFSI evolves into a nitrogen lone pair. In the meantime, the N lone pair of the (MeDalphos) ligand turns into a σ_{AuN} bond. The other d(Au) orbitals remain unchanged, in line with Au(I) to Au(III) oxidation (Figure S7).[18] For Selectfluor, the orbital redistribution and F^+ transfer occurs similarly, but earlier, when the Au–F distance reaches ~ 2.7 Å (Figures S8 and S9).[18]

Reactivity of the organo Au(III) fluoride complexes. The ability of MeDalphos to trigger Au(I) to Au(III) oxidation with mild oxidative fluorinating agent and to stabilize the ensuing organo Au(III) fluoride complexes prompted us to explore their reactivity. First, the potential of the obtained [(MeDalphos)Au(Ar)F]$^+$ complexes to act as model substrates in oxidative Au(I)/Au(III) cross-couplings was investigated. A variety of such catalytic transformations have been proposed to occur by oxidative fluorination of the Au(I) centre, followed by fluorine-assisted transmetalation and reductive elimination.[3,21,23] To probe the ability of the herein reported organo Au(III) fluorides to participate in such elementary steps, the mesityl complex **1e** was chosen as model system, due to its excellent thermal stability which allowed for facile manipulation and NMR monitoring.

No reaction was observed upon mixing **1e** with 1-phenyl-2-trimethylsilylacetylene at room temperature. However, heating to 80ºC for 8 hours afforded the coupling product in 53% yield (Scheme 4). With the trimethylsilyl cyanide TMSCN, the cross-coupling was found to proceed at significantly lower temperature, likely due to the more polarized Si–C(sp) bond. Within 2.5 hours at room temperature, mesityl cyanide was formed in good yield (80 %) alongside with (MeDalphos)AuCN **2**. Leaving the solution overnight resulted in the formation of colourless crystals suitable for X-ray diffraction analysis which enabled unambiguous confirmation of the structure of the gold(I) by-product. The mesityl complex **1e** was then substituted by the electron-deprived 2,6-difluorophenyl complex **1f**. The transmetalation with TMSCN still proceeded smoothly at room temperature to afford the corresponding benzonitrile in 71%

yield. Similar to what was previously observed for aryl–CN reductive eliminations at Au(III), the reaction proceeds more slowly with the electron-poor aryl group.[12,24] This electronic effect may be rationalized by the more ionic character of the Au–C bond formed with electron-deprived aryl groups, which increases the bond strength and decreases the driving force for reductive elimination.[25] When comparing the reaction between TMSCN and **1f** with that of the corresponding *trans* complex previously reported by Nevado *et al*,[12] it is observed that both the transmetalation and reductive elimination steps proceed slower with the contra-thermodynamic complex **1f**.[18] Besides electronic effects, we surmise that the high steric dissymmetry of the MeDalphos ligand comes into play. Thus, the organo Au(III) fluorides obtained by ligand-enabled oxidative fluorination readily engage into transmetalation/reductive elimination with C(sp)-based nucleophiles, demonstrating them to be relevant models for the Au(III) fluoride intermediates proposed in oxidative Au(I)/Au(III) catalytic cross-coupling reactions.

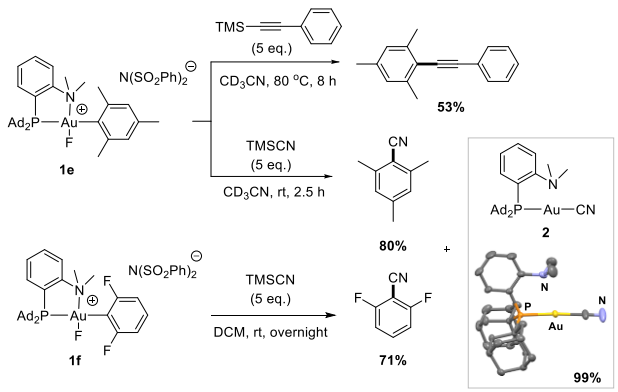

Scheme 4. Fluorine-assisted transmetalation of Au(III) fluorides with TMSC≡CPh and TMSCN. The latter resulted in the formation of (MeDalphos)AuCN **2** as Au(I) by-product. Yields based on ^{1}H NMR with diethyl terephthalate as internal standard or ^{19}F NMR with $PhCF_3$ as internal standard. Molecular structure of complex **2**. For sake of clarity, the hydrogen atoms are omitted. Ellipsoids are shown at 50% probability. Selected bond distances (in Å) and angles (in °): P–Au 2.303(1), NMe_2–Au 2.861(2), Au–C 2.000(2), P–Au–C 176.55(6).

A noteworthy aspect of the complexes prepared herein is the presence of both a fluoride and an organic group at Au(III). Hence, it was questioned whether direct reductive elimination (without transmetalation) is possible to forge C–F bonds. Aryl–F coupling is a highly challenging but attractive transformation,[26] given the abundance and significance of aryl fluoride derivatives within pharmaceuticals and agrochemicals.[27] While C(sp^2)–F reductive elimination is thermodynamically favoured due to the high C–F bond strength (DFT calculations support this assertion, *vide infra*),[28] the associated kinetic barrier is usually prohibitively high.[26,28,29] Because of its extreme electronegativity, fluorine forms highly

polarized M–F bonds, which significantly reduces electron density and orbital overlap as required for C–F reductive elimination to proceed.

The intrinsic difficulty associated with aryl–F coupling at transition metals has long hampered experimental observation. The first landmark study, by Ritter and co-workers, dates only from 2008.[30] Since then, the field has attracted considerable attention and several breakthroughs have been reported in recent years, with late transition metals (in particular palladium) and bismuth.[30-36] These developments have mainly focused on bringing the metal (or metaloid) centre to high oxidation state, such as Pd(IV), Pt(IV) or Bi(V), from which the C–F reductive elimination is comparatively more favoured.[30-32,36] The use of bulky ligands to force coordinatively unsaturated coordination environment at Pd(II) has also proven to be successful to promote aryl–F reductive elimination.[33,34] It is also worth noting that aryl–Cu(III)–F species have been proposed as key intermediates by Ribas *et al* in Ullmann-type halogen exchange at copper.[37]

Despite these achievements, the field is still in its infancy and much remains to be done to eventually make C(sp^2)–F reductive elimination a general, efficient and practical way to prepare aryl fluorides. In this context, we surmised that the [(MeDalphos)Au(Ar)F]$^+$ complexes may be inclined to undergo C–F coupling. Indeed, since the main obstacle on C(sp^2)–F reductive elimination is the high electronegativity of fluorine and polarized M–F bond, the transformation may be favoured with gold, the most electronegative transition metal. Incidentally, a few examples of C(sp^3)–F reductive eliminations have been observed by Toste and co-workers from Au(III) alkyl difluoride complexes.[9] Based on kinetic measurements and DFT studies, these reactions were proposed to take place from transient cationic three-coordinate [(IPr)Au(R)F]$^+$ intermediates. As for aryl–F coupling at Au(III), it was invoked once by Ribas and co-workers, to account for the fluorination of macrocyclic aryl halides mediated by Au(I),[38] but to the best of our knowledge, this process has never been directly evidenced experimentally. The mesityl complex **1e** was again chosen as model and we investigated its thermal behaviour, with the hope to promote C(sp^2)–F reductive elimination (Scheme 5). The targeted transformation only occurred when heating to 120 ºC. After 3 hours, **1e** was completely consumed and fluoro mesitylene was formed in a low 15% yield (based on ^{19}F NMR spectroscopy). To ensure the reaction is not induced by ambient light, it was performed in the dark and the same result was obtained. Changing the solvent to MeCN or the counterion of **1e** did not result in improved yields. Instead, no reaction or only decomposition was observed upon heating (Table S1).[18] Similar tests were performed with the 2,6-difluorophenyl complex **1f** but no sign of C–F reductive elimination could be observed upon heating in this case.

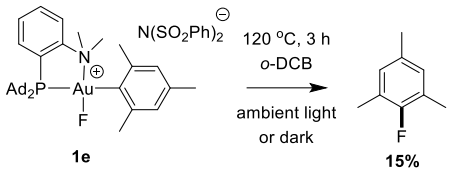

Scheme 5. Reductive elimination from the mesityl Au(III) fluoride complex 1e under thermal conditions. Yield based on ^{19}F NMR spectroscopy with $PhCF_3$ as internal standard.

To gain more insight, the energy profile for C(sp^2)–F reductive elimination from complex **1e** was computed (Figures 5 and S10). The reaction was found to be thermodynamically favoured by > 20 kcal/mol. Of note, the formed fluoro arene is η^2-bonded in the ensuing Au(I) π-complex.[39] The energy barrier computed for the C–F coupling at Au(III) is very high (~ 30 kcal/mol),[40] in agreement with the high thermal stability of **1e** and the low yield in fluoro mesitylene (most likely due to competing degradation paths). The transition state **TS** shows signs of growing 3-center $FAuC_{Mes}$ interaction. The C_{Mes}–Au–F bond angle is tight (53.71° *vs* 86.19° in **1e**), the Au–F bond is elongated by 10.1 % (2.139 Å *vs* 1.943 Å in **1e**) but the C_{Mes}–F distance remains long (1.921 Å *vs* 1.354 Å in Mes–F). The 2,6-difluorophenyl complex **1f** was also considered. Here, the activation barrier for C–F coupling at Au(III) was found to increase further to 41.3 kcal/mol (Figure S11).[18] This reflects the detrimental effect of the electron-withdrawing fluorine atoms on the aryl group towards reductive elimination (as observed in the aryl–CN coupling). This prohibitively high energy barrier also explains why no aryl–F coupling could be observed upon heating **1f**.

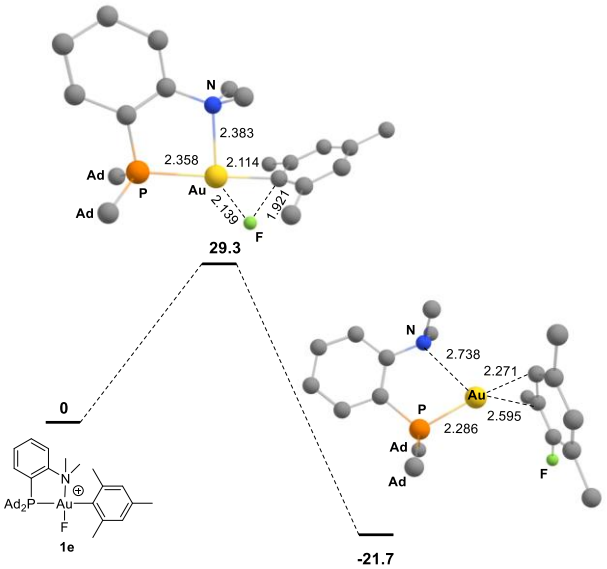

Figure 5. Gibbs free energy profile (ΔG in kcal/mol) for C(sp^2)–F reductive elimination from complex [(MeDalphos)Au(Mes)F]$^+$ 1e. Calculations carried out at SMD(MeCN)-B3PW91-D3(BJ)/SDD+f(Au),6-31G**//B3PW91-

D3(BJ)/SDD+f(Au),6-31G** level of theory. Main distances in Å and bond angle in °. For clarity, the hydrogen atoms and adamantyl (Ad) groups are omitted.

As C–F coupling from the aryl Au(III) fluoride complexes was found to be hardly possible under thermal conditions, we sought for an alternative method to induce the reductive elimination. We envisioned that the transformation could be promoted by irradiation instead of thermal means. A few recent reports have demonstrated that difficult reductive elimination reactions can be achieved this way with other transition metals. In 2017, MacMillan and coworkers have shown that cross-coupling between aryl halides and carboxylic acids can be performed by energy transfer from an excited iridium photocatalyst to an aryl Ni(II) carboxylate complex yielding the Ar–OCOR coupling products.[41] In addition, Iwasawa and co-workers demonstrated in 2022 that by using a photoactive acridine ligand instead of a photocatalyst, this challenging reductive elimination can also be achieved directly by irradiation of aryl Pd(II) carboxylate complexes (without external photosensitizer).[42] Considering the possibility to use light to promote Ar–F coupling at Au(III), complex **1e** was analysed by UV-VIS absorption spectroscopy. It shows a broad absorption peak at λ_{max} ~ 327 nm (Figure 6a). To shed light into the associated electronic transition, TD-DFT calculations were carried out at SMD(MeCN)-CAM-B3LYP/SDD+f(Au), 6-31G** (other atoms)//B3PW91-D3(BJ)/SDD+f(Au), 6-31G** (other atoms) level of theory (Table S7 and Figure S12).[18] The lowest-energy absorption maximum was found at λ 332 nm (oscillator strength *f* 0.046). It is mainly associated with electronic excitation from the HOMO to the LUMO, with an energy gap of 3.73 eV. The HOMO corresponds to the π^{b1} orbital of the aromatic substituent (Mes), while the LUMO is centered on the N–Au–F fragment and combines anti-bonding σ^*_{AuN} and σ^*_{AuF} orbitals (Figure 6c). The simulated absorption spectrum shows a second band at λ 306 nm (oscillator strength *f* 0.434), associated with an electronic transition from the HOMO–2 (localized on the P–Au–C_{Mes} fragment, combining σ_{AuP} and σ_{AuC} orbitals) to the LUMO (Figure S13).[18] These two transitions nicely match with the broad absorption band observed experimentally and suggest that the LUMO of complex **1e** could be accessed by irradiation, from which reductive elimination may occur. To this end, we tested irradiation at 365 nm in DCM and observed complete consumption of the Au(III) complex after 2 hours at room temperature with formation of fluoro mesitylene in a moderate, but significantly improved 45% yield (Figure 6b). This outcome showed the feasibility of light-induced reductive elimination to achieve reductive elimination at Au(III). Here, C(sp^2)–F coupling proceeds by direct irradiation of the aryl Au(III) fluoride complex, without the use of any photoactive ligand or external photocatalyst.[41,42]

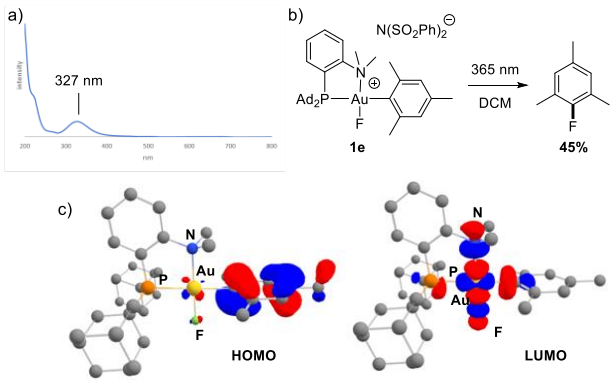

Figure 6. a) UV-VIS spectrum of complex 1e in MeCN. b) Reductive elimination from 1e upon irradiation at 365 nm in DCM resulting in fluoro mesitylene (yield based on ^{19}F NMR spectra with $PhCF_3$ as internal standard). c) HOMO and LUMO orbitals of complex 1e computed at B3PW91-D3(BJ)/SDD+f(Au),6-31G** (other atoms) level of theory (cutoff: 0.05).

Given the promising result obtained upon irradiation of **1e** in DCM at 365 nm, the conditions were varied to try to optimize the efficiency of the reaction (Scheme 6). Changing the solvent to MeCN resulted in an improved yield of 55%. Using higher-energy light sources proved detrimental (only 24% yield at best when irradiating at 312 or 254 nm). When lower-energy blue LEDs ($\lambda \sim 450$ nm) were utilized, a significant improvement was achieved. Reactions conducted in MeCN at this wavelength provided the C–F coupling product in an excellent 90% yield. The broad absorbance of complex **1e** with a tail up to *ca* 450 nm may explain that even visible light is able to trigger the transformation. Under these conditions, the (MeDalphos)Au$N(SO_2Ph)_2$ complex **3** was observed as the sole organometallic by-product and its structure was confirmed by single-crystal X-ray diffraction analysis. While complex **3** also formed in the reactions employing alternative solvents and higher-energy irradiation, it was not the exclusive by-product. Finally, the impact of the counteranion was examined with **1e-BF_4** and **1e-Cl**. In both cases, good yields were obtained, *albeit* slightly lower compared to **1e**, indicating a minimal impact of the anion on the light-induced reductive elimination. The irradiation of **1e** was then carried out at –20 °C, resulting in similar yields as under ambient temperature, consistent with the reductive elimination to occur from excited states of **1e**.

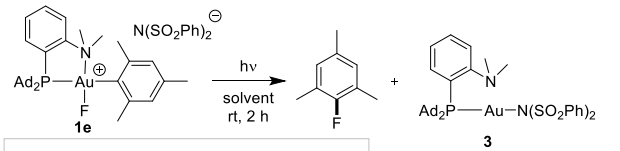

Solvent	Light source	Yield
DCM	254nm	10%
MeCN	254nm	13%
DCM	312nm	14%
MeCN	312nm	24%
DCM	365nm	45%
MeCN	365nm	55%
DCM	Blue LEDs	56%
MeCN	**Blue LEDs**	**90%**
MeCN	Blue LEDs	89% (–20°C)
MeCN	Blue LEDs	78% (from **1e.BF$_4$**)
MeCN	Blue LEDs	70% (from **1e.Cl**)

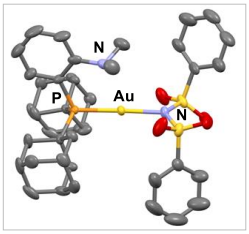

Scheme 6. Light-induced reductive elimination of complex **1e** under various conditions. Yields based on ^{19}F NMR spectroscopy with $PhCF_3$ as internal standard. Molecular structure of the (MeDalphos)Au$N(SO_2Ph)_2$ complex **3** obtained as by-product. For sake of clarity, the hydrogen atoms are omitted. Ellipsoids at 50% probability. Selected bond distances (in Å) and angles (in °): P–Au 2.244(1), NMe_2–Au 2.866(3), Au–$N(SO_2Ph)_2$ 2.092(2), P–Au–N 176.63(8).

In the thermal reaction of complexes **1e** and **1f** with TMSCN, the electronic nature of the aryl substituent was found to noticeably influence the rate of the C(sp^2)–CN coupling. We were thus curious to see how the light-induced C(sp^2)–F reductive elimination behaves and to this end, we irradiated the 2,6-difluorophenyl complex **1f** (Scheme 7). No C–F coupling was observed using blue LEDs in this case. This may be due to the blue-shift of the absorption maximum experienced by **1f** (λ_{max} ~ 310 nm *vs* λ_{max} ~ 327 nm for **1e**, Figure S2).[18] However, better results were obtained using higher-energy light sources, with 45% yield of the aryl–F coupling product when irradiating at 254 nm. At this point, the question arises as to whether the light-induced C(sp^2)–F reductive elimination observed with **1e** and **1f** is specific to the "contra-thermodynamic" form of aryl Au(III) fluorides or also possible with the corresponding ground-state structure. For this purpose, the F *trans* to P isomer of the 2,6-difluorophenyl complex **1f-*trans*** was prepared by oxidative addition of the corresponding aryl iodide followed by halide exchange with AgF, as previously reported (Figure 1b).[12] When this complex was irradiated at 365 nm, the C(sp^2)–F coupling product was obtained in 71% yield, showing that the light-induced reductive elimination from aryl Au(III) fluoride complexes is general and works beyond "contra-thermodynamic" complexes. ^{19}F NMR monitoring of two parallel photochemical reactions (MeCN, λ 365 nm) revealed that **1f-*trans*** reacts about 2 times faster than **1f**.[18]

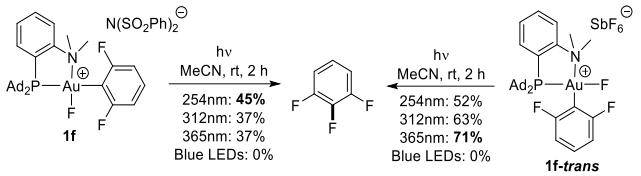

Scheme 7. Light-induced reductive eliminations from Au(III) fluoride complexes 1f and 1f-*trans*. Yields are based on ^{19}F NMR spectroscopy with $PhCF_3$ as internal standard.

Conclusion

The hemilabile MeDalphos ligand was shown to enable oxidative fluorination of Au(I) complexes. The reaction works with a wide range of sp, sp^2 and sp^3-hybridized organic groups at gold and various "F^+" sources (NFSI and Selectfluor, as well as *N*-fluoro pyridinium and XeF_2). The N atom of MeDalphos stabilizes the resulting Au(III) fluoride complex thanks to tetracoordination and it directs the F^+ transfer to gold in its *trans* position, resulting in "contra-thermodynamic" Au(III) fluoride complexes. The oxidative fluorination of Au(I), which is commonly proposed as the first elementary step in numerous catalytic transformations, has thus been experimentally authenticated and investigated in-depth computationally for the first time.

The thereby obtained aryl Au(III) fluoride complexes proved active in fluorine-assisted transmetalation/reductive elimination with C(sp) nucleophiles, leading to $C(sp^2)$–C(sp) coupling reactions mimicking the reaction sequence envisioned in catalytic transformations. Furthermore, the aryl Au(III) fluoride complexes were found to undergo challenging $C(sp^2)$–F reductive eliminations. While thermal means induce essentially decomposition, with only small amounts of C–F coupling, the direct irradiation of aryl Au(III) fluoride complexes with UV-visible light afforded the corresponding aryl fluorides in good yields under mild conditions (room temperature or even below).

It is worth noting that while the combination of light and gold has attracted significant interest,[4] most efforts have focused on promoting the oxidation of Au(I) centres, as this was considered to be the bottleneck for Au(I)/Au(III) redox chemistry until recently. Now that several ways have been developed to efficiently promote Au(I) to Au(III) oxidation,[1,3,4,6] the situation is somewhat reversed and the limiting step may be reductive elimination.[43] The results obtained with complexes **1e,f(-*trans*)** suggest that light-induced reductive elimination holds much potential to achieve challenging coupling reactions at gold and might even enable new ones.[44]

Other hemilabile ligands than MeDalphos recently reported to trigger oxidative addition to Au(I)[5o,5p,43] may promote oxidative fluorination and are certainly worth considering and investigating. Careful assessment of the ligand impact on this transformation as well as on the subsequent

transmetalation/cross-coupling and photo-induced C–F reductive elimination steps would provide useful insight to optimize ligand design and improve synthetic efficiency.

ASSOCIATED CONTENT

Supporting Information.

The Supporting Information is available free of charge at XXX.

Experimental and computational details, analytical data,

NMR spectra and cartesian coordinates (PDF)

Optimized Cartesian coordinates (XYZ)

AUTHOR INFORMATION

Corresponding Author

Didier Bourissou − Laboratoire Hétérochimie Fondamentale et Appliquée − LHFA UMR 5069, CNRS/Université de Toulouse, UPS, 31062 Toulouse Cedex 09, France

orcid.org/0000-0002-0249-1769

Email: didier.bourissou@univ-tlse3.fr

Authors

David Vesseur − Laboratoire Hétérochimie Fondamentale et Appliquée − LHFA UMR 5069, CNRS/Université de Toulouse, UPS, 31062 Toulouse Cedex 09, France

Shuo Li − Laboratoire Hétérochimie Fondamentale et Appliquée − LHFA UMR 5069, CNRS/Université de Toulouse, UPS, 31062 Toulouse Cedex 09, France

Sonia Mallet-Ladeira − Institut de Chimie de Toulouse − UAR 2599 − 118 Route de Narbonne, 31062 Toulouse Cedex 09 France

Karinne Miqueu − CNRS/Université de Pau et des Pays de l'Adour, E2S-UPPA, Institut des Sciences Analytiques et de Physico-Chimie pour l'Environnement et les Matériaux − IPREM UMR 5254, 64053 Pau Cedex 09, France

orcid.org/0000-0002-5960-1877

Author Contributions

The manuscript was written through contributions of all authors. All authors have given approval to the final version of the manuscript.

Notes

The authors declare no competing financial interest.

ACKNOWLEDGMENTS

Financial support from the Centre National de la Recherche Scientifique, the Université de Toulouse, the Agence Nationale de la Recherche (ANR-19-CE07-0037) and the Chinese Scholarship Council (PhD fellowship to S.L.) is gratefully acknowledged. The NMR service of ICT, UAR 2599 (Pierre Lavedan) is acknowledged for assistance with the variable-temperature NMR experiments. Thanks are due to Romaric Lenk (LHFA) for preliminary experiments on ligand-enabled oxidative fluorination of Au(I), to György Szalóki (LHFA) for assistance with cyclic voltammetry, to Saloua Chelli-Lakhdar for assistance with UV-vis spectroscopy and to Sami Lakhdar (LHFA) for insightful discussions. The "Direction du Numérique" of the Université de Pau et des Pays de l'Adour and the Mésocentre de Calcul Intensif Aquitain (MCIA) are acknowledged for the support of computational facilities. This work was also granted access to the HPC resources of IDRIS under the allocation 2022/2023-[AD010800045R1/AD010800045R2] made by GENCI.

REFERENCES

1. Huang, B.; Hu, M.; Toste, F. D. Homogeneous gold redox chemistry: organometallics, catalysis, and beyond. *Trends chem.* **2020**, *2* (8), 707–720, https://doi.org/10.1016/j.trechm.2020.04.012.

2. For selected references, see: a) Zhang, G.; Cui, L.; Wang, Y.; Zhang, L. Homogeneous gold-catalyzed oxidative carboheterofunctionalization of alkenes. *J. Am. Chem. Soc.* **2010**, *132* (5), 1474–1475, https://doi.org/10.1021/ja909555d; b) Melhado, A. D.; Brenzovich Jr, W. E.; Lackner, A. D.; Toste, F. D. Gold-catalyzed three-component coupling: oxidative oxyarylation of alkenes. *J. Am. Chem. Soc.* **2010**, *132* (26), 8885–8887, https://doi.org/10.1021/ja1034123; c) Brenzovich Jr., W. E.; Benitez, D.; Lackner, A. D.; Shunatona, H. P.; Tkatchouk, E.; Goddard III, W.A.; Toste, F. Gold-Catalyzed Intramolecular Aminoarylation of Alkenes: C−C Bond Formation through Bimolecular Reductive Elimination. *Angew. Chem. Int. Ed.* **2010**, *49* (32), 5519–5522, https://doi.org/10.1002/anie.201002739; d) Ball, L. T.; Green, M.; Lloyd-Jones, G. C.; Russell, C. A. Arylsilanes: Application to gold-catalyzed oxyarylation of alkenes. *Org. lett.* **2010**, *12* (21), 4724–4727, https://doi.org/10.1021/ol1019162; e) Ball, L. T.; Lloyd-Jones, G. C.; Russell, C. A. Gold-catalyzed direct arylation. *Science* **2012**, *337* (6102), 1644–1648, https://doi.org/10.1126/science.1225709; f) Cambeiro, X. C.; Ahlsten, N.; Larrosa, I.; Au-catalyzed cross-coupling of arenes via double C–H activation. *J. Am. Chem. Soc.* **2015**, *137* (50), 15636–15639, https://doi.org/10.1021/jacs.5b10593; g) Corrie, T. J.; Ball, L. T.; Russell, C. A.; Lloyd-Jones, G. C.; Au-catalyzed biaryl coupling to generate 5-to 9-membered rings: turnover-limiting reductive elimination versus π-complexation. *J. Am. Chem. Soc.* **2017**, *139* (1), 245–254, https://doi.org/10.1021/jacs.6b10018; h) Hofer, M.; Genoux, A.; Kumar, R.; Nevado, C. Gold-Catalyzed Direct Oxidative Arylation with Boron Coupling Partners. *Angew. Chem. Int. Ed.* **2017**, *56* (4), 1021–1025, https://doi.org/10.1002/anie.201610457; i) Hofer, M.; de Haro, T.; Gómez-Bengoa, E.; Genoux, A.; Nevado, C. Oxidant speciation and anionic ligand effects in the gold-catalyzed oxidative coupling of arenes and alkynes. *Chem. Sci.* **2019**, *10* (36), 8411–8420, https://doi.org/10.1039/C9SC02372K; j) Li, W.; Yuan, D.; Wang, G.; Zhao, Y.; Xie, J.; Li, S.; Zhu, C. Cooperative Au/Ag dual-catalyzed cross-dehydrogenative biaryl coupling: reaction development and mechanistic insight. *J. Am. Chem. Soc.* **2019**, *141* (7), 3187–3197, https://doi.org/10.1021/jacs.8b12929; k) Fang, S.; Han, J.; Zhu, C.; Li, W. Xie, J.; Gold-catalyzed four-component multifunctionalization of alkynes. *Nat. Commun.* **2023**, *14*, 3551, https://doi.org/10.1038/s41467-023-39243-5; l) Shiri, F.; Ariafard, A. Mechanistic details for oxidative addition of $PhICl_2$ to gold(I) complexes. *Chem. Commun.* **2023**, *59* (31), 4668–4671, https://doi.org/10.1039/D3CC00543G.

3. For reviews, see: a) Hopkinson, M. N.; Gee, A. D.; Gouverneur, V. Gold catalysis and fluorine. *Isr. J. Chem.* **2010**, *50* (5-6), 675–690, https://doi.org/10.1002/ijch.201000078; b) Hopkinson, M. N. Gee, A. D. Gouverneur, V. Au^{I}/Au^{III} Catalysis: An Alternative Approach for C–C Oxidative Coupling. *Chem. Eur. J.* **2011**, *17* (30), 8248–8262,

https://doi.org/10.1002/chem.201100736; c) Wegner, H. A.; Auzias, M. Gold for C–C Coupling Reactions: A Swiss-Army-Knife Catalyst?. *Angew. Chem. Int. Ed.* **2011**, *50* (36), 8236–8247, https://doi.org/10.1002/anie.201101603; d) Banerjee, S.; Bhoyare, V. W.; Patil, N. T. Gold and hypervalent iodine (III): liaisons over a decade for electrophilic functional group transfer reactions. *Chem. Commun.* **2020**, *56* (18), 2677–2690, https://doi.org/10.1039/D0CC00106F.

4. For reviews, see: a) Hopkinson, M. N.; Tlahuext-Aca, A.; Glorius, F. Merging visible light photoredox and gold catalysis. *Acc. Chem. Res.* **2016**, *49* (10), 2261–2272, https://doi.org/10.1021/acs.accounts.6b00351; b) Akram, M. O.; Banerjee, S.; Saswade, S. S.; Bedi, V.; Patil, N. T. Oxidant-free oxidative gold catalysis: the new paradigm in cross-coupling reactions. *Chem. Commun.* **2018**, *54* (79), 11069–11083, https://doi.org/10.1039/C8CC05601C; c) Witzel, S.; Hashmi, A. S. K.; Xie, J. Light in gold catalysis. *Chem. Rev.* **2021**, *121* (14), 8868–8925, https://doi.org/10.1021/acs.chemrev.0c00841.

5. For *o*-carboranyl P^P-chelating ligands, see: a) Joost, M.; Zeineddine, A.; Estevez, L.; Mallet−Ladeira, S.; Miqueu, K.; Amgoune, A.; Bourissou, D. Facile oxidative addition of aryl iodides to gold (I) by ligand design: bending turns on reactivity. *J. Am. Chem. Soc.* **2014**, *136* (42), 14654–14657, https://doi.org/10.1021/ja506978c; b) Joost, M.; Estévez, L.; Miqueu, K.; Amgoune, A.; Bourissou, D. Oxidative addition of carbon–carbon bonds to gold. *Angew. Chem. Int. Ed.* **2015**, *54* (17), 5236-5240, https://doi.org/10.1002/anie.201500458; For MeDalphos-type ligands, see: c) Zeineddine, A.; Estévez, L.; Mallet-Ladeira, S.; Miqueu, K.; Amgoune, A.; Bourissou, D. Rational development of catalytic Au (I)/Au (III) arylation involving mild oxidative addition of aryl halides. *Nat. Commun.* **2017**, *8* , 565, https://doi.org/10.1038/s41467-017-00672-8; d) Messina, M. S.; Stauber, J. M.; Waddington, M. A.; Rheingold, A. L.; Maynard, H. D.; Spokoyny, A. M. Organometallic gold (III) reagents for cysteine arylation. *J. Am. Chem. Soc.* **2018**, *140* (23), 7065–7069, https://doi.org/10.1021/jacs.8b04115; e) Rodriguez, J.; Zeineddine, A.; Carrizo, E. D. S.; Miqueu, K.; Saffon-Merceron, N.; Amgoune, A.; Bourissou, D. Catalytic Au(I)/Au(III) arylation with the hemilabile MeDalphos ligand: unusual selectivity for electron-rich iodoarenes and efficient application to indoles. *Chem. Sci.* **2019**, *10* (30), 7183–7192, https://doi.org/10.1039/C9SC01954E; f) Stauber, J. M.; Qian, E. A.; Han, Y.; Rheingold, A. L.; Král, P.; Fujita, D.; Spokoyny, A. M. An organometallic strategy for assembling atomically precise hybrid nanomaterials. *J. Am. Chem. Soc.* **2020**, *142* (1), 327–334, https://doi.org/10.1021/jacs.9b10770; g) Rodriguez, J.; Tabey, A.; Mallet-Ladeira, S.; Bourissou, D. Oxidative additions of alkynyl/vinyl iodides to gold and gold-catalyzed vinylation reactions triggered by the MeDalphos ligand. *Chem. Sci.* **2021**, *12* (22), 7706-7712, https://doi.org/10.1039/D1SC01483H; h) Stauber, J. M.; Rheingold, A. L.; Spokoyny, A. M. Gold(III) Aryl Complexes as Reagents for Constructing Hybrid Peptide-Based Assemblies via Cysteine *S*-Arylation. *Inorg. Chem.* **2021**, *60* (7), 5054–5062, https://doi.org/10.1021/acs.inorgchem.1c00087; i) Chintawar, C. C.; Bhoyare, V. W.; Mane, M. V.; Patil, N. T.; Enantioselective Au(I)/Au(III) redox catalysis enabled by chiral (P,N)-ligands. *J. Am. Chem. Soc.* **2022**, *144* (16), 7089–7095, https://doi.org/10.1021/jacs.2c02799; j) McDaniel, J. W.; Stauber, J. M.; Doud, E. A.; Spokoyny, A. M., Murphy, J. M. An Organometallic Gold(III) Reagent for ^{18}F Labeling of Unprotected Peptides and Sugars in Aqueous Media. *Org. Lett.* **2022**, *24* (28), 5132–5136, https://doi.org/10.1021/acs.orglett.2c01965; k) Montgomery. H. R.; Messina, M. S.; Doud, E. A.; Spokoyny, A. M.; Maynard. H. D. Organometallic S-arylation Reagents for Rapid PEGylation of Biomolecules. *Bioconjugate Chem.* **2022**, *33* (8), 1536–1542, https://doi.org/10.1021/acs.bioconjchem.2c00280; For alternative N^N, C^N and P^N ligands, see: l) Chu, J.; Munz, D.; Jazzar, R.; Melaimi, M.; Bertrand, G. Synthesis of hemilabile cyclic (alkyl)(amino) carbenes (CAACs) and applications in organometallic chemistry. *J. Am. Chem. Soc.* **2016**, *138* (25), 7884–7887, https://doi.org/10.1021/jacs.6b05221; m) Harper, M. J.; Arthur, C. J.; Crosby, J.; Emmett, E. J.; Falconer, R. L.; Fensham-Smith, A. J.; Gates, P. J.; Leman, T.; McGrady, J. E.; Bower, J. F.; Russell, C. A. Oxidative addition, transmetalation, and reductive elimination at a 2, 2′-bipyridyl-ligated gold center. *J. Am. Chem. Soc.* **2018**, *140* (12), 4440–4445, https://doi.org/10.1021/jacs.8b01411; n) Cadge, J. A.; Sparkes, H. A.; Bower, J. F. Russell, C. A. Oxidative addition of alkenyl and alkynyl iodides to a Au^{I} complex. *Angew. Chem. Int. Ed.* **2020**, *59* (16), 6617–6621, https://doi.org/10.1002/anie.202000473; o) Scott, S. C.; Cadge, J. A.; Boden, G. K.; Bower, J. F.; Russell, C. A. A Hemilabile NHC-Gold Complex and its Application to the Redox Neutral 1, 2-Oxyarylation of Feedstock Alkenes. *Angew. Chem. Int. Ed.* **2023**, *62* (23), e202301526, https://doi.org/10.1002/anie.202301526; p) Gao, P.; Xu, J.; Zhou, T.; Liu, Y.; Bisz, E.; Dziuk, B.; Lalancette, R.; Szostak, R.; Zhang, D.; Szostak, M. L-Shaped Heterobidentate Imidazo[1,5-a]pyridin-3-ylidene (N,C)-Ligands for Oxidant-Free Au^{I}/Au^{III} Catalysis. *Angew. Chem. Int. Ed.* **2023**, *62* (23), e202218427, https://doi.org/10.1002/anie.202218427; q) Font, P.; Valdés, H.; Guisado-Barrios, G.; Ribas, X.; Hemilabile MIC^N ligands allow oxidant-free Au(III)/Au(III) arylation-lactonization of γ-alkenoic acids. *Chem. Sci.* **2022**, *13* (32), 9351–9360, https://doi.org/10.1039/D2SC01966C.

6. For reviews, see: a) Font, P.; Ribas, X. Fundamental Basis for Implementing Oxidant-Free Au(I)/Au(III) Catalysis. *Eur. J. Inorg. Chem.* **2021**, (26), 2556–2569, https://doi.org/10.1002/ejic.202100301; b) McCallum, T. Heart of gold: enabling ligands for oxidative addition of haloorganics in Au (I)/Au(III) catalysed cross-coupling reactions. *Org. Biomol. Chem.* **2023**, *21* (8), 1629–1646, https://doi.org/10.1039/D3OB00002H.

7. a) Wolf, W. J.; Toste, F. D. "The Chemistry of Gold Fluoride Complexes." *PATAI'S Chemistry of Functional Groups*, **2009**, 1–18, https://doi.org/10.1002/9780470682531.pat0819; b) Miró, J.; del Pozo, C. Fluorine and gold: A fruitful partnership. *Chem. Rev.* **2016**, *116* (19), 11924–11966, https://doi.org/10.1021/acs.chemrev.6b00203.

8. Mankad, N. P.; Toste, F. D. C−C Coupling Reactivity of an Alkylgold(III) Fluoride Complex with Arylboronic Acids. *J. Am. Chem. Soc.* **2010**, *132* (37), 12859–12861, https://doi.org/10.1021/ja106257n.

9. Mankad, N. P.; Toste, F. D. C (sp^3)–F reductive elimination from alkylgold(III) fluoride complexes. *Chem. Sci.* **2012**, *3* (1), 72–76, https://doi.org/10.1039/C1SC00515D.

10. Additionally, Menjón and coworkers have shown in 2018 that the anionic bistrifluoromethyl Au(I) complex can be oxidized with XeF_2 and that the resulting *trans*-$[(F_3C)_2AuF_2]^-$ complex can exchange its fluorides with other halides and cyanide: Pérez-Bitrián, A.; Baya, M.; Casas, J. M.; Martín, A.; Menjón, B. Orduna, J. An Organogold(III) Difluoride with a *trans* Arrangement. *Angew. Chem. Int. Ed.* **2018**, 57 (22), 6517–6521, https://doi.org/10.1002/anie.201802379.

11. Kumar, R.; Linden, A.; Nevado, C. Evidence for Direct Transmetalation of Au^{III}–F with Boronic Acids. *J. Am. Chem. Soc.* **2016**, *138* (42), 13790–13793, https://doi.org/10.1021/jacs.6b07763.

12. Genoux, A. Biedrzycki, M. Merino, E. Rivera-Chao, E. Linden, A. Nevado, C. Synthesis and Characterization of Bidentate (P^N)Gold(III) Fluoride Complexes: Reactivity Platforms for Reductive Elimination Studies. *Angew. Chem. Int. Ed.* **2021**, *60* (8), 4164–4168, https://doi.org/10.1002/anie.202009359.

13. Fluorine-assisted transmetalation has also been reported with (C,C,N) pincer Au(III) fluoride complexes: a) Kumar, R.; Linden, A.; Nevado, C. Luminescent (N^C^C) gold (III) complexes: stabilized gold(III) fluorides. *Angew. Chem. Int. Ed.* **2015**, *54* (48), 14287–14290, https://doi.org/10.1002/ange.201505533; b) Beucher, H.; Kumar, S.; Kumar, R.; Merino, E.; Hu, W. H.; Stemmler, G.; Cuesta-Galisteo, S.; González, J. A.; Bezinge, L.; Jagielski, J.; Shih, C. J.; Nevado, C. Phosphorescent κ^3-(N^C^C)-Gold (III) Complexes: Synthesis, Photophysics, Computational Studies and Application to Solution-Processable OLEDs. *Chem. Eur. J.* **2020**, *26* (72), 17604–17612, https://doi.org/10.1002/chem.202003571.

14. For other stable L_3AuF, $LAuF_3$ and $(L_2AuF_2)^+$ complexes, see: a) Winston, M. S.; Wolf, W. J.; Toste, F. D. Halide-dependent mechanisms of reductive elimination from gold(III). *J. Am. Chem. Soc.* **2015**, *137* (24), 7921–7928, https://doi.org/10.1021/jacs.5b04613; b) Ellwanger, M. A. Steinhauer, S. Golz, P. Beckers, H. Wiesner, A. Braun-Cula, B. Braun, T. Riedel, S. Taming the High Reactivity of Gold(III) Fluoride: Fluorido Gold(III) Complexes with N-Based Ligands. *Chem. Eur. J.* **2017**, *23* (54), 13501–13509, https://doi.org/10.1002/chem.201702663; c) Ellwanger, M. A.; Steinhauer, S.; Golz, P.; Braun, T.; Riedel, S. Stabilization of Lewis Acidic AuF_3 as an N-Heterocyclic Carbene Complex: Preparation and Characterization of $[AuF_3(SIMes)]$. *Angew. Chem. Int. Ed.* **2018**, *57* (24), 7210–7214, https://doi.org/10.1002/anie.201802952; d) Albayer, M.; Corbo, R.; Dutton, J. L. Well defined difluorogold(III) complexes supported by N-ligands. *Chem. Commun.* **2018**, *54* (50), 6832–6834, https://doi.org/10.1039/C8CC02535E; e) Winter, M.; Ellwanger, M. A.; Limberg, N.; Pérez-Bitrián, A.; Voßnacker, P.; Steinhauer, S.; Riedel, S. Reactivity of $[AuF_3(SIMes)]$: Pathway to Unprecedented Structural Motifs. *Chem. Eur. J.* **2023**, *29* (51), e202301684, https://doi.org/10.1002/chem.202301684.

15. Kleinhans, G.; Chan, A. K. W.; Leung, M. Y.; Liles, D. C.; Fernandes, M. A.; Yam, V. W. W.; Fernandez, I.; Bezuidenhout, D. I. Synthesis and Photophysical Properties of T-Shaped Coinage-Metal Complexes. *Chem. Eur. J.* **2020**, *26* (31), 6993–6998, https://doi.org/10.1002/chem.202000726.

16. Rachor, S. G.; Ahrens, M.; Braun, T. Conversion of a Au^I Fluorido Complex into an *N*-Fluoroamido Derivative: N−F versus Au−N Reactivity. *Angew. Chem. Int. Ed.* **2022**, *61* (52), e202212858, https://doi.org/10.1002/anie.202212858.

17. a) Navarro, M.; Tabey, A.; Szaloki, G.; Mallet-Ladeira, S. Bourissou, D.; Stable Au(III) Complexes Bearing Hemilabile P^N and C^N Ligands: Coordination of the Pendant Nitrogen upon Oxidation of Gold. *Organometallics*, **2021**, *40* (11), 1571–1576, https://doi.org/10.1021/acs.organomet.1c00258; b) Szalóki, G.; Babinot, J.; Martin-Diaconescu, V.; Mallet-Ladeira, S.; García-Rodeja, Y.; Miqueu, K.; Bourissou, D. Ligand-enabled oxidation of gold(I) complexes with *o*-quinones. *Chem. Sci.* **2022**, *13* (35), 10499–10505, https://doi.org/10.1039/D2SC03724F; c) Rodriguez, J.; Vesseur, D.; Tabey, A.; Mallet-Ladeira, S.; Miqueu, K. Bourissou, D.; Au(I)/Au(III) catalytic allylation involving π-allyl Au(III) complexes. *ACS Catal.* **2022**, *12* (2), 993-1003, https://doi.org/10.1021/acscatal.1c04580.

18. See Supporting Information for details.

19. Yamamoto, K.; Li, J.; Garber, J. A.; Rolfes, J. D.; Boursalian, G. B.; Borghs, J. C.; Genicot, C.; Jacq, J.; van Gastel, M.; Neese, F.; Ritter, T. Palladium-catalysed electrophilic aromatic C–H fluorination. *Nature* **2018**, *554* (7693), 511–514, https://doi.org/10.1038/nature25749.

20. For discussions on *trans* effects in Au(III) complexes, see: a) Rocchigiani, L.; Fernandez-Cestau, J.; Chambrier, I.; Hrobárik, P.; Bochmann, M. Unlocking structural diversity in gold(III) hydrides: Unexpected interplay of *cis*/*trans*-influence on stability, insertion chemistry, and NMR chemical shifts. *J. Am. Chem. Soc.* **2018**, *140* (26), 8287–8302, https://doi.org/10.1021/jacs.8b04478; b) Rocchigiani, L.; Bochmann, M. Recent advances in gold(III) chemistry: structure, bonding, reactivity, and role in homogeneous catalysis. *Chem. Rev.* **2020**, *121* (14),8364–8451, https://doi.org/10.1021/acs.chemrev.0c00552; c) Holmsen, M. S. M.; Nova, A.; Tilset, M. Cyclometalated (N,C) Au (III) Complexes: The Impact of *Trans* Effects on Their Synthesis, Structure, and Reactivity. Accounts of Chemical Research. *Acc. Chem. Res.* **2023**, *56* (24), 3654–3664, https://doi.org/10.1021/acs.accounts.3c00595.

21. a) Qian, D.; Zhang, J. Au(I)/Au(III)-catalyzed Sonogashira-type reactions of functionalized terminal alkynes with arylboronic acids under mild conditions. *Beilstein J. Org. Chem.* **2011**, *7* (1), 808–812, https://doi.org/10.3762/bjoc.7.92; b) Leyva-Perez, A.; Doménech, A.; Al-Resayes, S. I.; Corma, A. Gold redox catalytic cycles for the oxidative coupling of alkynes. *ACS. Catal.* **2012**, *2* (1), 121–126, https://doi.org/10.1021/cs200532c; c) Leyva-Pérez, A.; Doménech-Carbó, A.; Corma, A. Unique distal size selectivity with a digold catalyst during alkyne homocoupling. *Nat. Commun.* **2015**, *6*, 6703, https://doi.org/10.1038/ncomms7703.

22. a) Knizia, G. Intrinsic atomic orbitals: An unbiased bridge between quantum theory and chemical concepts. *J. Chem. Theory Comput.* **2013**, *9* (11), 4834–4843, https://doi.org/10.1021/ct400687b; b) Knizia, G.; Klein, J. E. Electron flow in reaction mechanisms–revealed from first principles. A*ngew. Chem. Int. Ed.* **2015**, *54* (18), 5518–5522, https://doi.org/10.1002/anie.201410637.

23. For F^+-promoted gold-catalyzed heteroarylation of alkenes, see: a) Brenzovich Jr., W. E.; Benitez, D.; Lackner, A. D.; Shunatona, H. P.; Tkatchouk, E.; Goddard III, W.A.; Toste, F. D. Gold-Catalyzed Intramolecular Aminoarylation of Alkenes: C−C Bond Formation through Bimolecular Reductive Elimination. *Angew. Chem. Int. Ed.* **2010**, *49* (32), 5519–5522, https://doi.org/10.1002/anie.201002739; b) Melhado, A. D.; Brenzovich Jr, W. E.; Lackner, A. D.; Toste, F. D. Gold-catalyzed three-component coupling: oxidative oxyarylation of alkenes. *J. Am. Chem. Soc.* **2010**, *132* (26), 8885–8887, https://doi.org/10.1021/ja1034123; c) Zhang, G.; Cui, L.; Wang, Y.; Zhang, L. Homogeneous gold-catalyzed oxidative carboheterofunctionalization of alkenes. *J. Am. Chem. Soc.* **2010**, *132* (5), 1474–1475, https://doi.org/10.1021/ja909555d.

24. Genoux, A.; González, J. A.; Merino, E.; Nevado, C. Mechanistic Insights into $C(sp^2)$−C(sp)N Reductive Elimination from Gold(III) Cyanide Complexes. *Angew. Chem. Int. Ed.* **2020**, *59* (41), 1433–7851, https://doi.org/10.1002/anie.202005731.

25. For related considerations on isoelectronic Pd(II) complexes, see: Hartwig, J. F. Electronic effects on reductive elimination to form carbon−carbon and carbon−heteroatom bonds from palladium(II) complexes. *Inorg. Chem.* **2007**, *46* (6), 1936–1947, https://doi.org/10.1021/ic061926w.

26. a) Campbell, M. G.; Ritter, T.; Modern carbon–fluorine bond forming reactions for aryl fluoride synthesis. *Chem. Rev.* **2015**, *115* (2), 612–633, https://doi.org/10.1021/cr500366b; b) Neumann, C. N.; Ritter, T. Late-stage fluorination: fancy novelty or useful tool? *Angew. Chem. Int. Ed.* **2015**, *54* (11), 3216–3221, https://doi.org/10.1002/anie.201410288; c) Sather, A. C.; Buchwald, S. L. The evolution of Pd^0/Pd^{II}-catalyzed aromatic fluorination. *Acc. Chem. Res.* **2016**, *49* (10), 2146–2157, https://doi.org/10.1021/acs.accounts.6b00247; d) Clark, J. H. Aromatic fluorination. CRC Press, **2018**, https://doi.org/10.1201/9781351069885; e) Krüll, J.; Heinrich, M. R. [^{18}F] Fluorine-Labeled Pharmaceuticals: Direct Aromatic Fluorination Compared to Multi-Step Strategies. *Asian J. Org. Chem.* **2019**, *8* (5), 576–590, https://doi.org/10.1002/ajoc.201800494.

27. a) Theodoridis, G. Fluorine-containing agrochemicals: an overview of recent developments. *Advances in Fluorine Science*. **2006**, *2*, 121–175, https://doi.org/10.1016/S1872-0358(06)02004-5; b) Zhou, Y.; Wang, J.; Gu, Z.; Wang, S.; Zhu, W.; Aceña, J. L.; Soloshonok, V. A.; Izawa, K.; Liu, H. Next generation of fluorine-containing pharmaceuticals, compounds currently in phase II–III clinical trials of major pharmaceutical companies: new structural trends and therapeutic areas. *Chem. Rev.* **2016**, *116* (2), 422–518, https://doi.org/10.1021/acs.chemrev.5b00392; c) Wang, Q.; Song, H.; Wang, Q. Fluorine-containing agrochemicals in the last decade and approaches for fluorine incorporation. *Chin. Chem. Lett.* **2022**, *33* (2), 626–642, https://doi.org/10.1016/j.cclet.2021.07.064; d) Jeschke, P. Recent developments in fluorine-containing pesticides. *Pest Manag Sci.* **2024**, https://doi.org/10.1002/ps.7921.

28. Luo, Y. R. Handbook of bond dissociation energies in organic compounds. CRC press. **2002**.

29. a) Furuya, T.; Klein, J. E. M. N.; Ritter, T. Carbon-fluorine bond formation for the synthesis of aryl fluorides. *Synthesis*, **2010**, 1804–1821, https://doi.org/10.1055/s-0029-1218742 ; b) Furuya, T.; Kamlet, A. S.; Ritter, T. Catalysis for fluorination and trifluoromethylation. *Nature* **2011**, *473* (7348), 470–477, https://doi.org/10.1038/nature10108.

30. Furuya, T.; Ritter, T. Carbon−fluorine reductive elimination from a high-valent palladium fluoride. *J. Am. Chem. Soc.* **2008**, *130* (31), 10060–10061, https://doi.org/10.1021/ja803187x.

31. Lee, E.; Kamlet, A. S.; Powers, D. C.; Neumann, C. N.; Boursalian, G. B.; Furuya, T.; Choi, D. C.; Hooker, J. M.; Ritter, T. A fluoride-derived electrophilic late-stage fluorination reagent for PET imaging. *Science* **2011**, *334* (6056), 639–642, https://doi.org/10.1126/science.1212625.

32. Ball, N. D.; Sanford, M. S. Synthesis and reactivity of a mono-σ-aryl palladium(IV) fluoride complex. *J. Am. Chem. Soc.* **2009**, *131* (11), 3796–3797, https://doi.org/10.1021/ja8054595.

33. Yandulov, D. V.; Tran, N. T. Aryl-fluoride reductive elimination from Pd(II): feasibility assessment from theory and experiment. *J. Am. Chem. Soc.* **2007**, *129* (5), 1342–1358, https://doi.org/10.1021/ja066930l.

34. Watson, D. A.; Su, M.; Teverovskiy, G.; Zhang, Y.; García-Fortanet, J.; Kinzel, T.; Buchwald, S. L. Formation of ArF from LPdAr(F): catalytic conversion of aryl triflates to aryl fluorides. *Science* **2009**, *325* (5948), 1661–1664, https://doi.org/10.1126/science.1178239.

35. Dubinsky-Davidchik, I.; Goldberg, I.; Vigalok, A.; Vedernikov, A. N. Selective Aryl–Fluoride Reductive Elimination from a Platinum(IV) Complex. *Angew. Chem. Int. Ed.* **2015**, *54* (42), 12447–12451, https://doi.org/10.1002/anie.201503116.

36. a) Planas, O.; Wang, F.; Leutzsch, M.; Cornella, J. Fluorination of arylboronic esters enabled by bismuth redox catalysis. *Science* **2020**, *367* (6475), 313–317, https://doi.org/10.1126/science.aaz2258; b) Planas, O.; Peciukenas, V.; Leutzsch, M.; Nöthling, N.; Pantazis, D. A.; Cornella, J. Mechanism of the Aryl–F Bond-Forming Step from Bi(V) Fluorides. *J. Am. Chem. Soc.* **2022**, 144, 14489–14504, https://doi.org/10.1021/jacs.2c01072.

37. a) Casitas, A. Canta, M.; Sola, M.; Costas, M.; Ribas, X. Nucleophilic Aryl Fluorination and Aryl Halide Exchange Mediated by a Cu^I/Cu^{III} Catalytic Cycle. *J. Am. Chem. Soc.* **2011**, *133* (48), 19386–19392, https://doi.org/10.1021/ja2058567; b) Ribas, X.; Guell, I. Cu(I)/Cu(III) catalytic cycle involved in Ullmann-type cross-coupling reactions. *Pure Appl. Chem.* **2014**, *86* (3), 345–360, https://doi.org/10.1515/pac-2013-1104; c) Dong, T.; Tsui, G. C. Construction of Carbon-Fluorine Bonds *via*

Copper-Catalyzed/-Mediated Fluorination Reactions. *Chem. Rec.* **2021**, *21* (12), 4015–4031, https://doi.org/10.1002/tcr.202100231.

38. Serra, J.; Whiteoak, C. J.; Acuña-Parés, F.; Font, M.; Luis, J. M.; Lloret-Fillol, J.; Ribas, X. Oxidant-Free Au(I)-Catalyzed Halide Exchange and Csp^2–O Bond Forming Reactions. *J. Am. Chem. Soc.* **2015**, *137* (41), 13389–13397, https://doi.org/10.1021/jacs.5b08756.

39. Blons, C.; Amgoune, A.; Bourissou, D. Gold(III) π complexes. *Dalton Trans.* **2018**, *47* (31), 10388–10393, https://doi.org/10.1039/C8DT01457D.

40. $\Delta G^{\neq}$ = 29.3 kcal/mol at SMD(MeCN)-B3PW91-D3(BJ)/SDD+f(Au),6-31G**//B3PW91-D3(BJ)/SDD+f(Au),6-31G** level of theory. Complementary calculations were performed to assess the impact of dispersion and counter-anion effects. $\Delta G^{\neq}$ varied by only 1–2 kcal/mol (Table S6).[18]

41. Welin, E. R.; Le, C.; Arias-Rotondo, D. M.; McCusker, J. K.; MacMillan, D. W. Photosensitized, energy transfer-mediated organometallic catalysis through electronically excited nickel(II). *Science* **2017**, *355* (6323), 380–385, 10.1126/science.aal2490.

42. Toriumi, N.; Inoue, T.; Iwasawa, N. Shining Visible Light on Reductive Elimination: Acridine–Pd-Catalyzed Cross-Coupling of Aryl Halides with Carboxylic Acids. *J. Am. Chem. Soc.* **2022**, *144* (42), 19592–19602, https://doi.org/10.1021/jacs.2c09318.

43. For example, Gagosz and co-workers have shown in a recent study that lowering the energy barrier for reductive elimination by just a few kcal/mol upon fine ligand tuning may enable to improve the yields of Au(I)/Au(III) alkoxy- and amido-arylations of alkenes by up to 20%. Muratov, K.; Zaripov, E.; Berezovski, M. V.; Gagosz, F. DFT-guided Development of Hemilabile (P^N) Ligands for Gold(I/III) RedOx Catalysis: Application to the Thiotosylation of Aryl Iodides. *J. Am. Chem. Soc.* **2024**, *146* (6), 3660–3674, https://doi.org/10.1021/jacs.3c08943.

44. For a previously reported light-induced reductive chloride elimination from Au(III), see: Park, G.; Karimi, M.; Liu, W. C.; Gabbaï, F. P.; Green-Light-Driven Reductive Elimination of Chlorine from a Carbene-Xanthylium Gold(III) Complex. *Angew. Chem. Int. Ed.* **2022**, *61* (31), e202206265, https://doi.org/10.1002/anie.202206265.